IJCSE International Journal of Computer Sciences and Engineering Open Access
Research Paper Vol.-6, Issue-9, Sept. 2018 E-ISSN: 2347-2693

Recognition of Complex Power Quality Disturbances Using Discrete Wavelet Transform and Fuzzy C-means Clustering

Umesh Kumar Sharma[1*], Tanuj Manglani[2]

[1,2]Department of Electrical Engineering, Yagyavalkya Institute of Technology, Jaipur, India

Available online at: www.ijcseonline.org

Accepted: 12/Sept/2018, Published: 30/Sept/2018

Abstract— This paper's approach based on discrete wavelet transform and Fuzzy c-means clustering for the detection and classification of the complex power quality disturbances. The complex power quality disturbances have been generated in MATLAB by various combinations of the mathematical models single stage power quality disturbances such as voltage sag, voltage swell, momentary interruption, oscillatory transient, impulsive transient, harmonics, notch and spike. The investigated complex power quality disturbances are (voltage sag + harmonics), (voltage swell + harmonics), (momentary interruption + harmonics), (oscillatory transient + voltage sag), (oscillatory transient + harmonics), (impulsive transient + voltage sag), (Impulsive Transient + harmonics) and (oscillatory Transient, Voltage Sag and Harmonics). The DWT based plots up to fourth level of decomposition of the voltage signal with complex PQ disturbance are used for the recognition of the complex PQ disturbances. The DWT based features have been given as input to the Fuzzy c-means clustering for classification purpose of the complex PQ disturbances. It is observed that the proposed algorithm is effective in the detection and classification of the complex power quality disturbances. The proposed approach has been implemented using the MATLAB codes.

Keywords—Power Quality, Complex power quality disturbance; Discrete wavelet transform; Fuzzy C-means clustering.

I. INTRODUCTION

Recently the electric power systems have been disturbed with unwanted variations in the voltage and current signal due to rapid industrialization of the world. The power quality (PQ) problems are basically due to disturbances which may occur in interconnected power system networks, which contain large numbers of power sources, transmission lines, transformers and other various types of loads. The expose of power system network to environmental disturbances like lightning strikes also produce power quality disturbances. Furthermore, nonlinear power electronic loads such as converters driven equipment which have become increasingly common in power system also produce PQ disturbances. Poor quality of power supply is also attributed due to various power line disturbances. In brief, PQ problems may cause system equipment malfunction; computer data loss and memory malfunction of sensitive loads such as computer, programmable logic controller controls, protection and relaying equipment; and erratic operation of electronic controls. Hence, Detection of Power Quality (PQ) is an essential service in today's aspects. Poor PQ shortens the life of load and can damage the load [1]. Therefore, it is necessary to take care of these power quality disturbances to supply good quality power to the customers [2]. Therefore, the cause and source of poor power quality must be known so that a suitable mitigation action may be initiated.

Techniques which are generally used in the extraction of features of disturbances from a large number of power signals for the analysis of power quality are fast Fourier transform (FFT) and the windowed Fourier transform whichcomprises of the short time Fourier transform (STFT), the wavelet transform (WT) and discrete wavelet transform (DWT) [3]. In [4] authors presented a wavelet transform based energy function approach technique for detection of some power quality (PQ) disturbances such as voltage sag, voltage flicker, voltage swell. In [5] authors has provided a broad scenario about popular techniques for power quality (PQ) analysis in electrical power systems such as the wavelet transform, the S-transform, the Gabor transform, and the Wigner distribution function. A scenario on constantly increasing the number and power of loads that pollute the electric network has been presented in [6] and for this a new technique called ''power quality analysis (PQAT)'' has been proved to be efficient in the identification of the loads. In [7], authors presents a heart disease diagnosing (HDD) system consists of a sensitive movement EMFiTM-film1 sensor installed under the upholstery of a chair using Bi-orthogonal wavelet transforms and artificial neural networks. In [8], during power swing for correct distance relay operation a new protection scheme is

introduced to identify symmetrical faults. This new protection scheme is used to identify symmetrical faults during power swing conditions based on mixture of S-Transform (ST) and Probabilistic Neural Network (PNN) methods. In [9], PQ events classifications are done using ANN with Hilbert Transform and it is found that RBFNN is the most efficient topology to perform the classification task.

II. GENERATION OF COMPLEX PQ DISTURBANCES

The investigated complex power quality disturbances have been generated using various combinations of the mathematical formulations of single stage power quality disturbances reported in [10]. These mathematical relations for the complex PQ disturbances have been modeled in MATLAB using the codes for the mathematical relations of single stage PQ disturbance reported in [10]. The formulated complex power quality disturbances include (voltage sag + harmonics), (voltage swell + harmonics), (momentary interruption + harmonics), (oscillatory transient + voltage sag), (oscillatory transient + harmonics), (impulsive transient + voltage sag), (Impulsive Transient + harmonics) and (oscillatory Transient, Voltage Sag and Harmonics).

III. PROPOSED METHODOLOGY

The following steps are employed for the recognition of complex power quality disturbances using the discrete wavelet transform and Fuzzy c-means clustering:-

- The signals with power quality disturbances which are complex in nature have been generated in MATLAB using mathematical models reported in [10].
- These signals with complex PQ disturbances have been decomposed using DWT up to level 4.
- Various plots such as approximation coefficient at fourth level of decomposition, detail coefficient at fourth level of decomposition, detail coefficient at third level of decomposition and detail coefficient at first level of decomposition have been obtained.
- Patterns of above mentioned plots have been analysed which helps for detection of various PQ disturbances.
- Features are extracted from the discrete wavelet transform based plots of the each complex PQ disturbance. These features are given as input to the Fuzzy c-means clustering for the classification purpose.
- The Fuzzy C-means clustering based scatter plots between two features taken at a time are used for the classification of single stage PQ disturbances. It has been observed that the four combinations of plots between cD1-cD2, cD4- cA4, cD4-cD3 and cD3-cD2 are found effective for FCM clustering based classification.

IV. SIMULATION RESULTS AND DISCUSSION

This section presents the simulation results related to the recognition of complex power quality disturbances using the discrete wavelet transform and Fuzzy c-means clustering. Various combinations of the single stage power quality disturbances such as pure sine wave, voltage sag, voltage swell, momentary interruption, flicker, harmonics, spike, notch, oscillatory transient and impulsive transient have been used to generate complex power quality disturbances investigated in this study. The voltage signal with complex power quality disturbance is decomposed using the discrete wavelet transform with db4 mother wavelet up to fourth level of the decomposition. The db4 mother wavelet is selected by testing the proposed algorithm with various types of the mother wavelet. It is observed that the results with high accuracy are obtained while using the db4 mother wavelet. The results are analyzed up to level four. The details coefficient at first level (cD1), detail coefficient at second level (cD2), detail coefficient at third level (cD3), detail coefficient at fourth level (cD4) and approximation coefficient at fourth level (cA4) of decomposition are analyzed for the detection of the complex power quality disturbances.

A. Voltage Sag with Harmonics

The voltage signal with voltage sag and harmonics is decomposed using discrete wavelet transform (DWT) up to fourth level of decomposition with db4 as mother wavelet. The voltage signal with sag and harmonics, approximation coefficient at fourth level of decomposition (cA4), detail coefficient at fourth level of decomposition (cD4), detail coefficient at third level of decomposition (cD3), detail coefficient at second level of decomposition (cD2) and detail coefficient at first level of decomposition (cD1) are illustrated in Fig. 1 (a), (b), (c), (d), (e) and (f) respectively.

It is observed from the detail coefficient cD1 of Fig. 1 (f) that there are high magnitude peaks at the time of start and end of the sag in the voltage signal. These high magnitude peaks will help to localize the voltage sag. The magnitude of the detail coefficients cD4, cD3 and cD2 decreases during the time period of the voltage sag as shown in Fig. 1 (c), (d) and (e) respectively. This decreased magnitude helps to recognize the sag in the voltage. The magnitude of approximation coefficient cA4 decreases during the time period of the voltage sag as shown in Fig. 1 (b) which indicates the presence of the sag in the voltage signal.

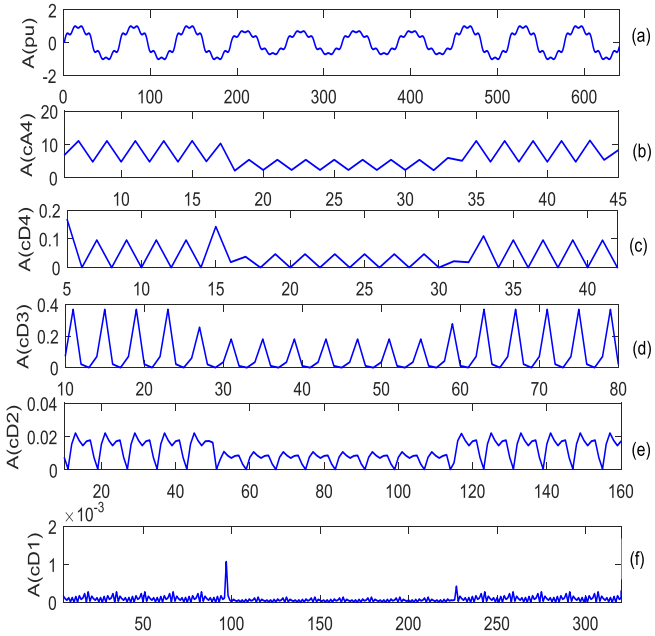

Fig. 1 Wavelet transform based decomposition of voltage signal with sag and harmonics (a) voltage signal with sag and harmonics (b) approximation coefficient at fourth level of decomposition (c) detail coefficient at fourth level of decomposition (d) detail coefficient at third level of decomposition (e) detail coefficient at second level of decomposition and (f) detail coefficient at first level of decomposition.

It is observed from the detail coefficient cD1 of Fig. 1 (f) that there is a regular pattern of the low magnitude ripples indicating the presence of the harmonics. It is also observed from the detail coefficient cD2 of Fig. 1 (e) that there is also a regular pattern of the peaks with flattened tops indicating the presence of harmonics in the voltage signal. The ripples of high magnitude observed in the detail coefficients cD4 and cD3 shown in Fig. 1 (c) and (d) respectively also indicates the presence of the harmonics in the voltage signal. The harmonics available in the voltage signal have not been detected in the approximation coefficient at fourth level of decomposition (cA4) as shown in Fig. 1 (b).

B. Voltage Swell with Harmonics

The voltage signal with voltage swell and harmonics is decomposed using discrete wavelet transform (DWT) up to fourth level of decomposition with db4 as mother wavelet. The voltage signal with swell and harmonics, approximation coefficient at fourth level of decomposition (cA4), detail coefficient at fourth level of decomposition (cD4), detail coefficient at third level of decomposition (cD3), detail coefficient at second level of decomposition (cD2) and detail coefficient at first level of decomposition (cD1) are illustrated in Fig. 2 (a), (b), (c), (d), (e) and (f) respectively.

It is observed from the detail coefficient cD1 of Fig. 2 (f) that there are high magnitude peaks at the times of start and end of the swell in the voltage signal. These high magnitude peaks will help to localize the voltage swell. The magnitude of the detail coefficients cD4, cD3 and cD2 increases during the time period of the voltage swell as shown in Fig. 2 (c), (d) and (e) respectively. This increased magnitude helps to recognize the swell in the voltage. The magnitude of approximation coefficient cA4 increases during the time period of the voltage swell as shown in Fig. 2 (b) which indicates the presence of the swell in the voltage signal.

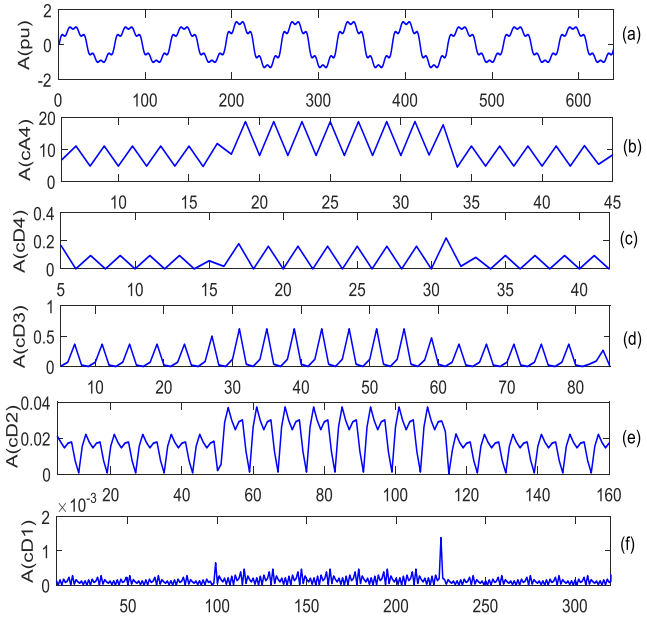

Fig. 2 Wavelet transform based decomposition of voltage signal with swell and harmonics (a) voltage signal with swell and harmonics (b) approximation coefficient at fourth level of decomposition (c) detail coefficient at fourth level of decomposition (d) detail coefficient at third level of decomposition (e) detail coefficient at second level of decomposition and (f) detail coefficient at first level of decomposition

It is observed from the detail coefficient cD1 of Fig. 2 (f) that there is a regular pattern of the low magnitude ripples indicating the presence of the harmonics. It is also observed from the detail coefficient cD2 of Fig. 2 (e) that there is also a regular pattern of the peaks with flattened tops indicating the presence of harmonics in the voltage signal. The ripples of high magnitude observed in the detail coefficients cD4 and cD3 shown in Fig. 2 (c) and (d) respectively also indicates the presence of the harmonics in the voltage signal. The harmonics available in the voltage signal have not been detected in the approximation coefficient at fourth level of decomposition (cA4) as shown in Fig. 2 (b).

C. Momentary Interruption with Harmonics

The voltage signal with momentary interruption and harmonics is decomposed using discrete wavelet transform (DWT) up to fourth level of decomposition with db4 as mother wavelet. The voltage signal with momentary interruption and harmonics, approximation coefficient at fourth level of decomposition (cA4), detail coefficient at fourth level of decomposition (cD4), detail coefficient at third level of decomposition (cD3), detail coefficient at second level of decomposition (cD2) and detail coefficient at first level of decomposition (cD1) are illustrated in Fig. 3 (a), (b), (c), (d), (e) and (f) respectively. It is observed from the detail coefficient cD1 of Fig. 3 (f) that there are high magnitude peaks at the time of start and end of the momentary interruption. These high magnitude peaks will help to localize the momentary interruption. Magnitude of the detail coefficients cD4, cD3 and cD2 decreases nearly to zero during time period of the momentary interruption as shown in Fig. 3 (c), (d) and (e) respectively. This decreased magnitude below 10% helps to recognize the momentary interruption. The magnitude of approximation coefficient cA4 also decreases below 10% during the time period of momentary interruption as shown in Fig. 3 (b) which indicates the presence of the momentary interruption in the voltage signal.

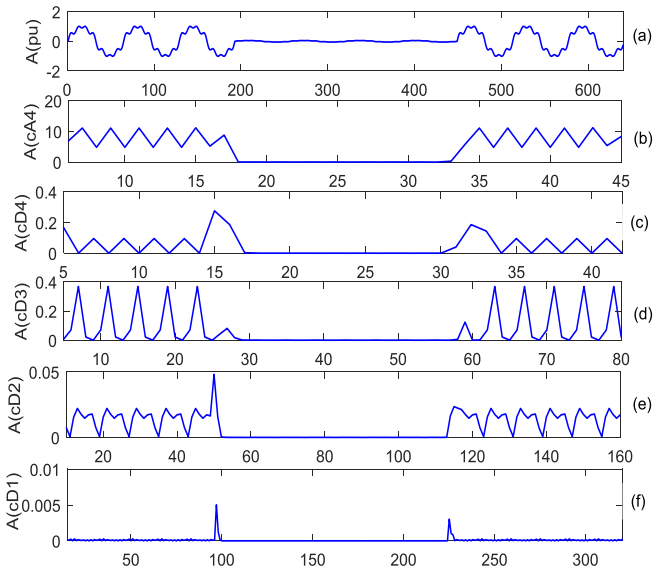

Fig. 3 Wavelet transform based decomposition of voltage signal with momentary interruption and harmonics (a) voltage signal with momentary interruption and harmonics (b) approximation coefficient at fourth level of decomposition (c) detail coefficient at fourth level of decomposition (d) detail coefficient at third level of decomposition (e) detail coefficient at second level of decomposition and (f) detail coefficient at first level of decomposition.

It is observed from the detail coefficient cD1 of Fig. 3 (f) that there is a regular pattern of the low magnitude ripples indicating the presence of the harmonics. This pattern is not significant during the period of the momentary interruption because the magnitude of the voltage signal is low for this period. It is also observed from the detail coefficient cD2 of Fig. 3 (e) that there is also a regular pattern of the peaks with flattened tops indicating the presence of harmonics in the voltage signal. This pattern is also not significant during the period of the momentary interruption because the magnitude of the voltage signal is low for this period. The ripples of high magnitude observed in the detail coefficients cD4 and cD3 shown in Fig. 3 (c) and (d) respectively also indicates the presence of the harmonics in the voltage signal. The harmonics available in the voltage signal have not been detected in the approximation coefficient at fourth level of decomposition (cA4) as shown in Fig. 3 (b).

D. Voltage Sag with Oscillatory Transient

The voltage signal with voltage sag and oscillatory transient is decomposed using discrete wavelet transform (DWT) up to fourth level of decomposition with db4 as mother wavelet. The voltage signal with sag and oscillatory transient, approximation coefficient at fourth level of decomposition (cA4), detail coefficient at fourth level of decomposition (cD4), detail coefficient at third level of decomposition (cD3), detail coefficient at second level of decomposition (cD2) and detail coefficient at first level of decomposition (cD1) are illustrated in Fig. 4 (a), (b), (c), (d), (e) and (f) respectively. Since the magnitude of the oscillatory transient is relatively high compared to the voltage sag, hence the sag in voltage is detected significantly in the approximation coefficient at level four (cA4) as shown in Fig. 4 (b) between samples numbers 25 to 38.

It is observed from the detail coefficient cD1 of Fig. 4 (f) that there are high magnitude peaks at the time of start and end of the oscillatory transient and relatively high magnitude during all other times of the oscillatory transient in the voltage signal (between samples 95 to 130). These high magnitude peaks will help to localize the oscillatory transient and combination of these high magnitude peaks and relatively high magnitude indicates the presence of the oscillatory transient in the voltage signal. It is also observed from the detail coefficient cD2 of Fig. 4 (e) that there are also high magnitude peaks at the time of start and end of the oscillatory transient and relatively high magnitude during all other times of the oscillatory transient in the voltage signal (between samples 50 to 68). These high magnitude peaks will also help to localize the oscillatory transient and combination of these high magnitude peaks and relatively high magnitude indicates the presence of the oscillatory transient in the voltage signal. The magnitude of the detail coefficients cD4 and cD3 shown in Fig. 4 (c) and (d) respectively also increases to high values during period for

which the oscillatory transient is present in the voltage signal. Hence, the significant changes observed in curves of all the detail coefficients indicate the presence of the oscillatory transient in the voltage signal. Minor changes are observed in the approximation coefficient shown in Fig. 6.4 (b) at the time of the oscillatory transient.

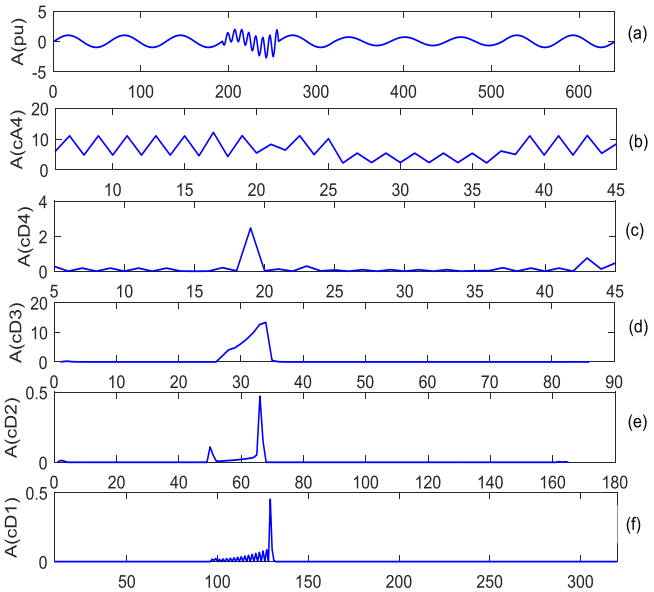

Fig. 4 Wavelet transform based decomposition of voltage signal with sag and oscillatory transient (a) voltage signal with sag and oscillatory transient (b) approximation coefficient at fourth level of decomposition (c) detail coefficient at fourth level of decomposition (d) detail coefficient at third level of decomposition (e) detail coefficient at second level of decomposition and (f) detail coefficient at first level of decomposition.

E. Momentary Interruption with Oscillatory Transient

The voltage signal with voltage sag and oscillatory transient is decomposed using discrete wavelet transform (DWT) up to fourth level of decomposition with db4 as mother wavelet. The voltage signal with momentary interruption and oscillatory transient, approximation coefficient at fourth level of decomposition (cA4), detail coefficient at fourth level of decomposition (cD4), detail coefficient at third level of decomposition (cD3), detail coefficient at second level of decomposition (cD2) and detail coefficient at first level of decomposition (cD1) are illustrated in Fig. 6.5 (a), (b), (c), (d), (e) and (f) respectively. Since the magnitude of the oscillatory transient is relatively high compared to the momentary interruption, hence the momentary interruption is detected significantly in the approximation coefficient at level four (cA4) as shown in Fig. 6.5 (b) between samples numbers 25 to 38 and also detected in the detail coefficient at level four (cD4) as shown in Fig. 6.5 (c) between samples numbers 25 to 38.

It is observed from the detail coefficient cD1 of Fig. 5 (f) that there are high magnitude peaks at the time of start and end of the oscillatory transient and relatively high magnitude during all other times of the oscillatory transient in the voltage signal (between samples 95 to 130). These high magnitude peaks will help to localize the oscillatory transient and combination of these high magnitude peaks and relatively high magnitude indicates the presence of the oscillatory transient in the voltage signal. It is also observed from the detail coefficient cD2 of Fig. 5 (e) that there are also high magnitude peaks at the time of start and end of the oscillatory transient and relatively high magnitude during all other times of the oscillatory transient in the voltage signal (between samples 50 to 68). These high magnitude peaks will also help to localize the oscillatory transient and combination of these high magnitude peaks and relatively high magnitude indicates the presence of the oscillatory transient in the voltage signal. The magnitude of the detail coefficients cD4 and cD3 shown in Fig. 5 (c) and (d) respectively also increases to high values during period for which the oscillatory transient is present in the voltage signal. Hence, the significant changes observed in curves of all the detail coefficients indicate the presence of the oscillatory transient in the voltage signal. Minor changes are observed in the approximation coefficient shown in Fig. 5 (b) at the time of the oscillatory transient.

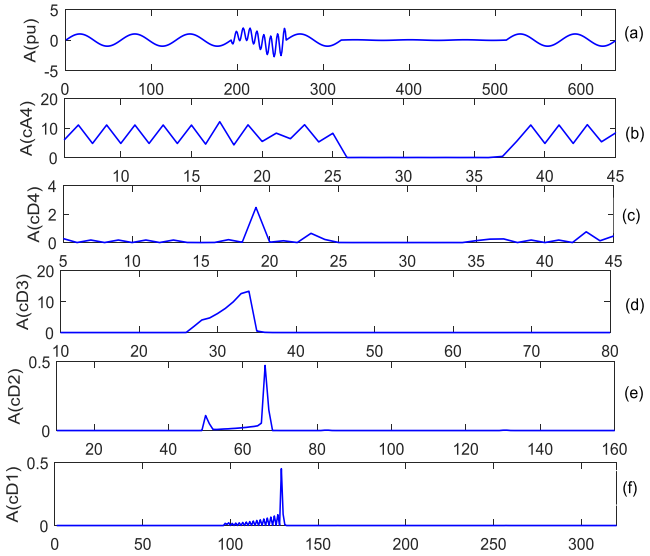

Fig. 5 Wavelet transform based decomposition of voltage signal with momentary interruption and oscillatory transient (a) voltage signal with momentary interruption and oscillatory transient (b) approximation coefficient at fourth level of decomposition (c) detail coefficient at fourth level of decomposition (d) detail coefficient at third level of decomposition (e) detail coefficient at second level of decomposition and (f) detail coefficient at first level of decomposition.

F. Harmonics with Oscillatory Transient

The voltage signal with harmonics and oscillatory transient is decomposed using discrete wavelet transform (DWT) up to fourth level of decomposition with db4 as mother wavelet. The voltage signal with momentary interruption and oscillatory transient, approximation coefficient at fourth level of decomposition (cA4), detail coefficient at fourth level of decomposition (cD4), detail coefficient at third level of decomposition (cD3), detail coefficient at second level of decomposition (cD2) and detail coefficient at first level of decomposition (cD1) are illustrated in Fig. 6 (a), (b), (c), (d), (e) and (f) respectively. It is observed from detail coefficient cD2 of Fig. 6 (e) that there is a regular pattern of the peaks with flattened tops indicating the presence of harmonics in the voltage signal. This pattern is not significant during the period of the momentary interruption because magnitude of the voltage signal is low for this period. The ripples of low magnitude observed in detail coefficients cD4 and cD3 shown in Fig. 6.6 (c) and (d) respectively also indicates presence of harmonics in the voltage signal. The harmonics available in the voltage signal have not been detected in the approximation coefficient at fourth level of decomposition (cA4) as shown in Fig. 6 (b).

It is observed from the detail coefficient cD1 of Fig. 6 (f) that there are high magnitude peaks at the time of start and end of the oscillatory transient and relatively high magnitude during all other times of the oscillatory transient in the voltage signal (between samples 125 to 170). These high magnitude peaks will help to localize the oscillatory transient and combination of these high magnitude peaks and relatively high magnitude indicates the presence of the oscillatory transient in the voltage signal. It is also observed from the detail coefficient cD2 of Fig. 6 (e) that there are also high magnitude peaks at the time of start and end of the oscillatory transient and relatively high magnitude during all other times of the oscillatory transient in the voltage signal (between samples 65 to 85). These high magnitude peaks will also help to localize the oscillatory transient and combination of these high magnitude peaks and relatively high magnitude indicates the presence of the oscillatory transient in the voltage signal. Magnitude of the detail coefficients cD4 and cD3 shown in Fig. 6 (c) and (d) respectively also increases to high values during period for which the oscillatory transient is present in the voltage signal. Hence, the significant changes observed in curves of all the detail coefficients indicate the presence of the oscillatory transient in the voltage signal. Minor changes are observed in the approximation coefficient shown in Fig. 6 (b) at the time of the oscillatory transient.

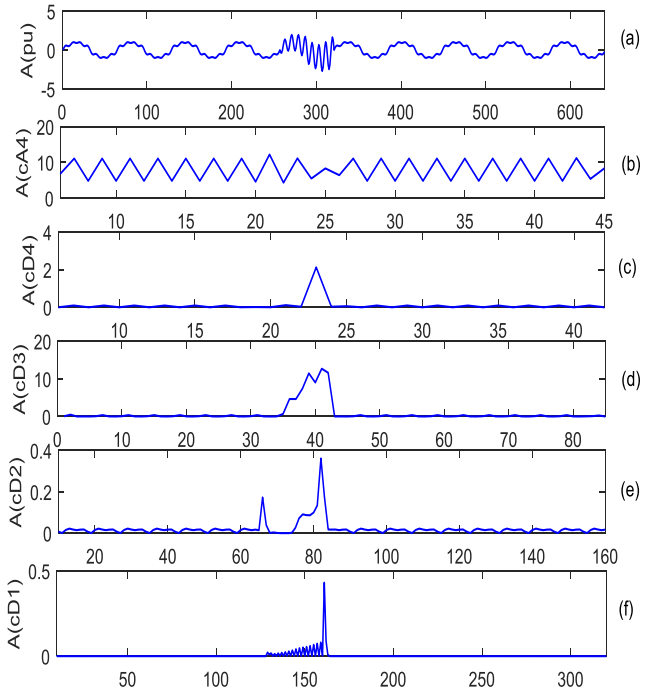

Fig. 6 Wavelet transform based decomposition of voltage signal with momentary interruption and oscillatory transient (a) voltage signal with momentary interruption and oscillatory transient (b) approximation coefficient at fourth level of decomposition (c) detail coefficient at fourth level of decomposition (d) detail coefficient at third level of decomposition (e) detail coefficient at second level of decomposition and (f) detail coefficient at first level of decomposition.

G. *Impulsive Transient with Voltage Sag*

The voltage signal with voltage sag and impulsive transient is decomposed using discrete wavelet transform (DWT) up to fourth level of decomposition with db4 as mother wavelet. The voltage signal with sag and impulsive transient, approximation coefficient at fourth level of decomposition (cA4), detail coefficient at fourth level of decomposition (cD4), detail coefficient at third level of decomposition (cD3), detail coefficient at second level of decomposition (cD2) and detail coefficient at first level of decomposition (cD1) are illustrated in Fig. 7 (a), (b), (c), (d), (e) and (f) respectively. Since magnitude of the impulsive transient is relatively high compared to the voltage sag, hence the sag in voltage is detected significantly in the approximation coefficient at level four (cA4) as shown in Fig. 7 (b) between samples numbers 25 to 38.

It is observed from the detail coefficient cD1 of Fig. 7 (f) that a sharp magnitude peak is observed at the time of occurrence of the impulsive transient. This high magnitude peak helps to recognize the presence of impulsive transient. It is also observed from the detail coefficient cD2 of Fig. 7

(e) that there is also a high magnitude peak at the time of occurrence of impulsive transient indicating the presence of the impulsive transient in the voltage signal. Magnitude of the detail coefficients cD4 and cD3 shown in Fig. 7 (c) and (d) respectively also increases to high values at the time of occurrence of impulsive transient. Hence, peaks of significant high magnitude indicate the presence of the impulsive transient in the voltage signal. A high magnitude peak observed in the approximation coefficient shown in Fig. 7 (b) also indicates the presence of the impulsive transient with the voltage signal.

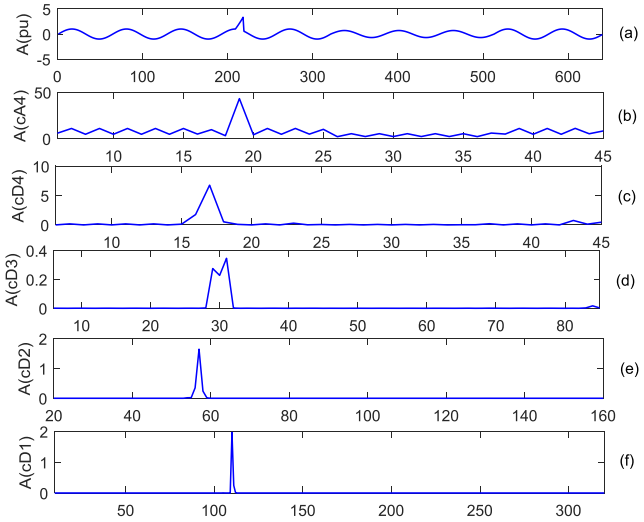

Fig. 7 Wavelet transform based decomposition of voltage signal with impulsive transient and sag (a) voltage signal with impulsive transient and sag (b) approximation coefficient at fourth level of decomposition (c) detail coefficient at fourth level of decomposition (d) detail coefficient at third level of decomposition (e) detail coefficient at second level of decomposition and (f) detail coefficient at first level of decomposition

H. Notch with Voltage Sag

The voltage signal with voltage sag and notches is decomposed using discrete wavelet transform (DWT) up to fourth level of decomposition with db4 as mother wavelet. The voltage signal with sag and notches, approximation coefficient at fourth level of decomposition (cA4), detail coefficient at fourth level of decomposition (cD4), detail coefficient at third level of decomposition (cD3), detail coefficient at second level of decomposition (cD2) and detail coefficient at first level of decomposition (cD1) are illustrated in Fig. 8 (a), (b), (c), (d), (e) and (f) respectively. The decreased magnitude of the voltage signal between sample numbers 18 to 34 of the approximation coefficient at level four (cA4) as shown in Fig. 8 (b) indicates the presence of the voltage sag. The voltage sag is also detected by the decreased magnitude of the detail coefficient cD4 between the samples number 18 to 34 as shown in Fig. 8 (c). During the sag period the magnitude of the detail coefficient cD3 also decreases slightly as shown in the Fig. 8 (d). Voltage sag is not detected from the curve of detail coefficients cD1 and cD2.

It is observed from the detail coefficient cD1 of Fig. 8 (f) that a sequence of ripples with sharp peaks is observed at the time of notches in the voltage signal. The sharp magnitude peaks help to recognize the presence of the notches in the voltage signal. It is also observed from the detail coefficient cD2 of Fig. 8 (e) that there is also a series of sharp magnitude peaks which also helps to recognize the presence of the notches in the voltage signal. Sharp magnitude peaks are also observed in the detail coefficients cD3 shown in Fig. 8 (d) at regular intervals indicating the presence of the notches in the voltage signal. The spikes are not detected from the detail coefficient (cD4) and approximation coefficient (cA3) shown in Fig. 8 (b) and (c) respectively.

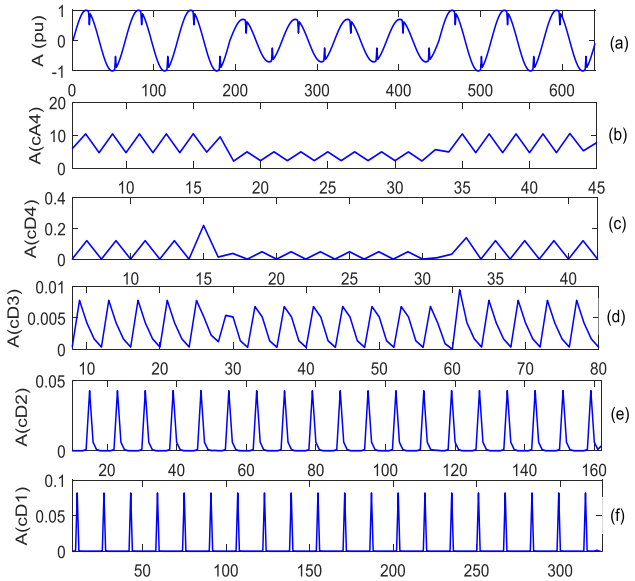

Fig. 8 Wavelet transform based decomposition of voltage signal with notch and oscillatory transient (a) voltage signal with notch and oscillatory transient (b) approximation coefficient at fourth level of decomposition (c) detail coefficient at fourth level of decomposition (d) detail coefficient at third level of decomposition (e) detail coefficient at second level of decomposition and (f) detail coefficient at first level of decomposition

I. Spike with Voltage Sag

The voltage signal with voltage sag and spikes is decomposed using discrete wavelet transform (DWT) up to fourth level of decomposition with db4 as mother wavelet. The voltage signal with sag and spikes, approximation coefficient at fourth level of decomposition (cA4), detail coefficient at fourth level of decomposition (cD4), detail coefficient at third level of decomposition (cD3), detail

coefficient at second level of decomposition (cD2) and detail coefficient at first level of decomposition (cD1) are illustrated in Fig. 9 (a), (b), (c), (d), (e) and (f) respectively. The decreased magnitude of the voltage signal between sample numbers 18 to 34 of the approximation coefficient at level four (cA4) as shown in Fig. 9 (b) indicates the presence of the voltage sag. The voltage sag is also detected by the decreased magnitude of the detail coefficient cD4 between the samples number 18 to 34 as shown in Fig. 9 (c). During the sag period the magnitude of the detail coefficient cD3 also decreases slightly as shown in the Fig. 9 (d). Voltage sag is not detected from the curve of detail coefficients cD1 and cD2.

It is observed from the detail coefficient cD1 of Fig. 9 (f) that a train of sharp peaks is observed at the time of spikes in the voltage signal. This train of sharp magnitude peaks help to recognize presence of spikes in the voltage signal. It is also observed from the detail coefficient cD2 of Fig. 9 (e) that there is also a train of sharp magnitude peaks which also helps to recognize the presence of the spikes in the voltage signal. High magnitude peaks are also observed in the detail coefficients cD3 shown in Fig. 9 (d) at regular intervals indicating the presence of the spikes in the voltage signal. The spikes are not detected from the detail coefficient (cD4) and approximation coefficient (cD3) shown in Fig. 9 (b) and (c) respectively.

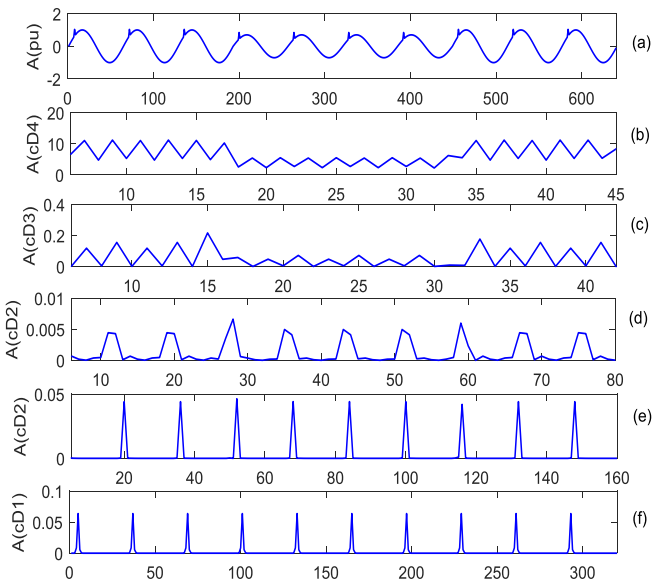

Fig. 9 Wavelet transform based decomposition of voltage signal with spike and sag (a) voltage signal with spike and sag (b) approximation coefficient at fourth level of decomposition (c) detail coefficient at fourth level of decomposition (d) detail coefficient at third level of decomposition (e) detail coefficient at second level of decomposition and (f) detail coefficient at first level of decomposition

J. Spike with Voltage Sag

The voltage signal with voltage sag, oscillatory transient and harmonics is decomposed using discrete wavelet transform (DWT) up to fourth level of decomposition with db4 as mother wavelet. The voltage signal with sag, harmonics and oscillatory transient, approximation coefficient at fourth level of decomposition (cA4), detail coefficient at fourth level of decomposition (cD4), detail coefficient at third level of decomposition (cD3), detail coefficient at second level of decomposition (cD2) and detail coefficient at first level of decomposition (cD1) are illustrated in Fig. 10 (a), (b), (c), (d), (e) and (f) respectively. Since the magnitude of the oscillatory transient is relatively high compared to the voltage sag, hence the sag in voltage is detected significantly in the approximation coefficient at level four (cA4) as shown in Fig. 10 (b) between samples numbers 25 to 38.

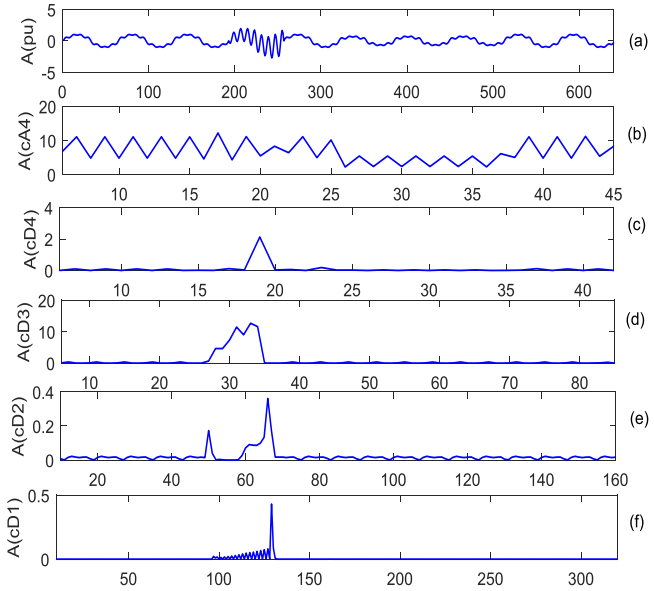

Fig. 10 Wavelet transform based decomposition of voltage signal with oscillatory transient, harmonics and sag (a) voltage signal with oscillatory transient, harmonics and sag (b) approximation coefficient at fourth level of decomposition (c) detail coefficient at fourth level of decomposition (d) detail coefficient at third level of decomposition (e) detail coefficient at second level of decomposition and (f) detail coefficient at first level of decomposition.

It is observed from the detail coefficient cD1 of Fig. 10 (f) that there are high magnitude peaks at the time of start and end of the oscillatory transient and relatively high magnitude during all other times of the oscillatory transient in the voltage signal (between samples 95 to 130). These high magnitude peaks will help to localize the oscillatory transient and combination of these high magnitude peaks and relatively high magnitude indicates the presence of the oscillatory transient in the voltage signal. It is also observed

from the detail coefficient cD2 of Fig. 10 (e) that there are also high magnitude peaks at the time of start and end of the oscillatory transient and relatively high magnitude during all other times of the oscillatory transient in the voltage signal (between samples 50 to 68). These high magnitude peaks will also help to localize the oscillatory transient and combination of these high magnitude peaks and relatively high magnitude indicates the presence of the oscillatory transient in the voltage signal. The magnitude of the detail coefficients cD4 and cD3 shown in Fig. 10 (c) and (d) respectively also increases to high values during period for which the oscillatory transient is present in the voltage signal. Hence, the significant changes observed in curves of all the detail coefficients indicate the presence of the oscillatory transient in the voltage signal. Minor changes are observed in the approximation coefficient shown in Fig. 10 (b) at the time of the oscillatory transient. It is observed from detail coefficient cD2 of Fig. 10 (e) that there is a regular pattern of the peaks with flattened tops indicating the presence of harmonics in the voltage signal. This pattern is not significant during the period of the momentary interruption because magnitude of the voltage signal is low for this period. The ripples of low magnitude observed in detail coefficients cD4 and cD3 shown in Fig. 10 (c) and (d) respectively also indicates presence of harmonics in the voltage signal. The harmonics available in the voltage signal have not been detected in the approximation coefficient at fourth level of decomposition (cA4) as shown in Fig. 10 (b).

V. FEATURES USED FOR THE CLASSIFICATION PURPOSE

The following features are used to plot the Fuzzy c-means clustering based scatter plots for classification of the single stage power quality disturbances.

F1=cA4=Values of approximation coefficient obtained at fourth level of decomposition of voltage signal with PQ disturbance using discrete wavelet transform.
F2=cD4=Values of detail coefficient obtained at fourth level of decomposition of voltage signal with PQ disturbance using discrete wavelet transform.
F3=cD3=Values of detail coefficient obtained at third level of decomposition of voltage signal with PQ disturbance using discrete wavelet transform.
F4=cD4=Values of detail coefficient obtained at second level of decomposition of voltage signal with PQ disturbance using discrete wavelet transform.
F5=t=Time duration of the disturbance signal.

VI. CLASSIFICATION USING FUZZY C-MEANS CLUSTERING

The Fuzzy C-means clustering based scatter plots between two features taken at a time are used for the classification of complex PQ disturbances. It has been observed that the four combinations of plots between cD1-cD2, cD4- cA4, cD4-cD3 and cD3-cD2 are found effective for FCM clustering based classification of complex PQ disturbances. These plots give different separate clusters of the data which helps to recognise and differentiate the complex power quality disturbances from each other with high accuracy. The scatter plots for all the disturbances are shown in Fig. 11. In all the figures related to the Fuzzy c-means clustering the following representation of the data is used D1: Voltage Sag with Harmonics, D2: Voltage Swell with Harmonics, D3: Momentary Interruption with Harmonics, D4: Voltage Sag with Oscillatory Transient, D5: Momentary Interruption with Oscillatory Transient, D6: Harmonics with Oscillatory Transient, D7: Impulsive Transient with Voltage Sag, D8: Notch with Voltage Sag, D9: Spike with Voltage Sag and D10: Oscillatory Transient, Voltage Sag and Harmonics.

It is observed from the scatter plots of the Fig. 11 that the data related to the complex PQ disturbances can be divided into two groups G1 and G2. The data related to the D1: Voltage Sag with Harmonics, D2: Voltage Swell with Harmonics, D3: Momentary Interruption with Harmonics, D8: Notch with Voltage Sag and D9: Spike with Voltage Sag is clustered together and can be included in the group G1. The data related to the D4: Voltage Sag with Oscillatory Transient, D5: Momentary Interruption with Oscillatory Transient, D6: Harmonics with Oscillatory Transient, D7: Impulsive Transient with Voltage Sag, and D10: Oscillatory Transient, Voltage Sag and Harmonics are clustered together and can be included in the group G2. The data include in the groups G1 and G2 can be classified further to distinguish the various PQ disturbances.

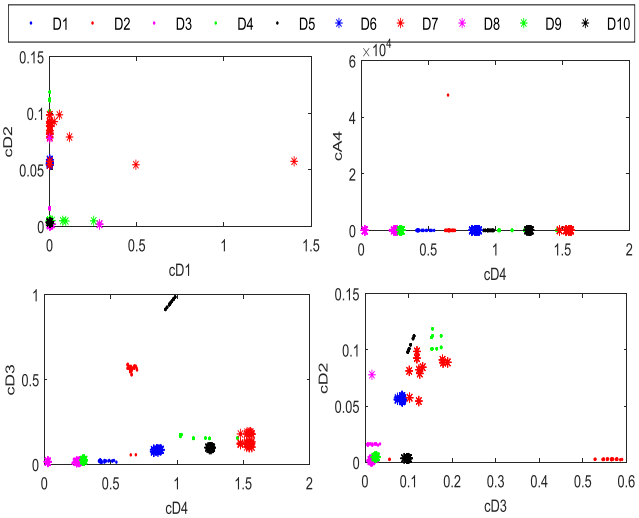

Fig. 11 Fuzzy c-means clustering of the complex PQ disturbances (a) cD1-cD2 plot (b) cD4-cA4 plot (c) cD4-cD3 plot and (d) cD3-cD2 plot used for classification of disturbances into subgroups G1 and G2.

The scatter plots of the related to the D1: Voltage Sag with Harmonics, D2: Voltage Swell with Harmonics, D3: Momentary Interruption with Harmonics, D8: Notch with Voltage Sag and D9: Spike with Voltage Sag and included in the group G1 are provided in the Fig. 12. It is observed from the Fig. 12 that depending on the clustering of the data, the data related to the PQ disturbances included in the groups G1 are divided into two groups G11 and G12.

It is observed from the Fig. 12 that data related to the D3: Momentary Interruption with Harmonics, D8: Notch with Voltage Sag and D9: Spike with Voltage Sag is clustered together and can be included in the groups G11. It is also observed that the data related to the D1: Voltage Sag with Harmonics, D2: Voltage Swell with Harmonics is clustered together and can be included in the group G12.

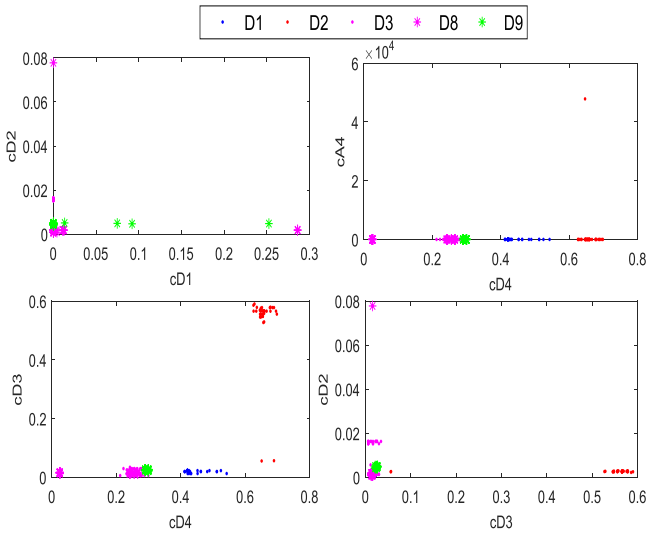

Fig. 12 Fuzzy c-means clustering of the single stage PQ disturbances of group G1 data (a) cD1-cD2 plot (b) cD4-cA4 plot (c) cD4-cD3 plot and (d) cD3-cD2 plot used for classification of disturbances.

The scatter plots of the disturbances related to the D3: Momentary Interruption with Harmonics, D8: Notch with Voltage Sag and D9: Spike with Voltage Sag is included in the group G11 are provided in the Fig. 13. It is observed from the scatter plots between the cD4 and cD3 as well as cD3 and cD2 are the most effective in the discrimination of the data related to the data groups D3, D8 and D9. However, all other scatter plots also indicate the effective classification of the complex PQ disturbances.

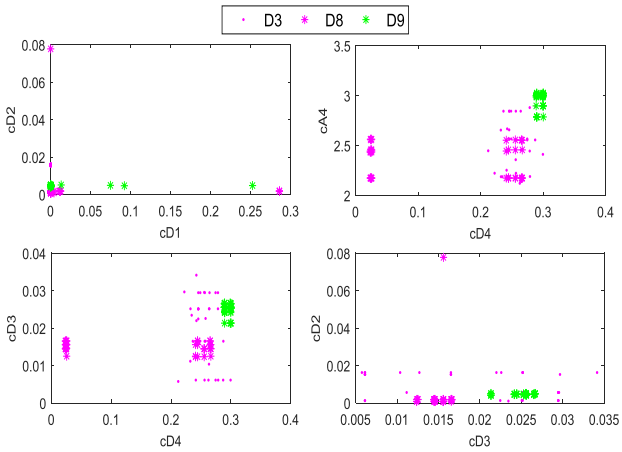

Fig. 13 Fuzzy c-means clustering of the single stage PQ disturbances of group G11 data (a) cD1-cD2 plot (b) cD4-cA4 plot (c) cD4-cD3 plot and (d) cD3-cD2 plot used for classification of disturbances.

The scatter plots of the PQ disturbances related to the D1: Voltage Sag with Harmonics, D2: Voltage Swell with Harmonics included in the group G12 is provided in the Fig. 14. It is observed from all the scatter plots of Fig. 14 are effective in the discrimination and classification of the complex PQ disturbances included in the group G12.

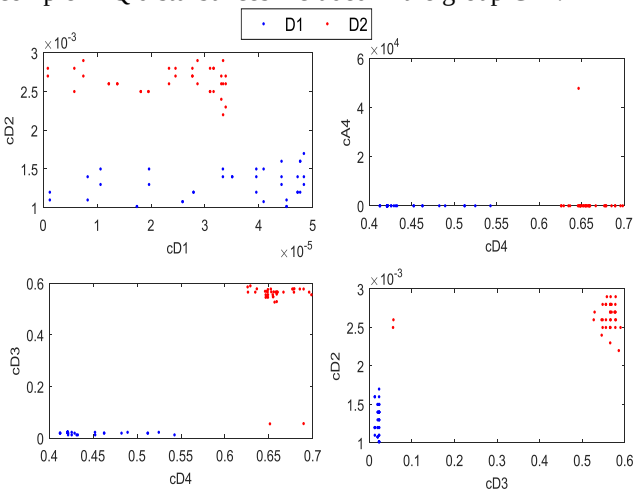

Fig. 14 Fuzzy c-means clustering of the single stage PQ disturbances of group G12 data (a) cD1-cD2 plot (b) cD4-cA4 plot (c) cD4-cD3 plot and (d) cD3-cD2 plot used for classification of disturbances.

The scatter plots of complex PQ disturbances related to the D4: Voltage Sag with Oscillatory Transient, D5: Momentary Interruption with Oscillatory Transient, D6: Harmonics with Oscillatory Transient, D7: Impulsive Transient with Voltage Sag, and D10: Oscillatory Transient, Voltage Sag and Harmonics included in the group G2 are provided in the Fig. 15. It is observed from the Fig. 15 that depending on the clustering of the data, the data related to the complex PQ

disturbances included in the groups G2 are divided into two groups G21 and G22. The data of PQ disturbances related to the D7: Impulsive Transient with Voltage Sag, and D10: Oscillatory Transient, Voltage Sag and Harmonics included are included in the group G21. The data related to the complex PQ disturbances D4: Voltage Sag with Oscillatory Transient, D5: Momentary Interruption with Oscillatory Transient, D6: Harmonics with Oscillatory Transient are included in the group G22.

The scatter plots of the disturbances related to the D7: Impulsive Transient with Voltage Sag, and D10: Oscillatory Transient, Voltage Sag and Harmonics included in the group G21 are provided in the Fig. 16. It is observed from the all the scatter plots that data related to all the D7: Impulsive Transient with Voltage Sag, and D10: Oscillatory Transient, Voltage Sag and Harmonics are clustered separately indicating that the effective classification of these disturbances.

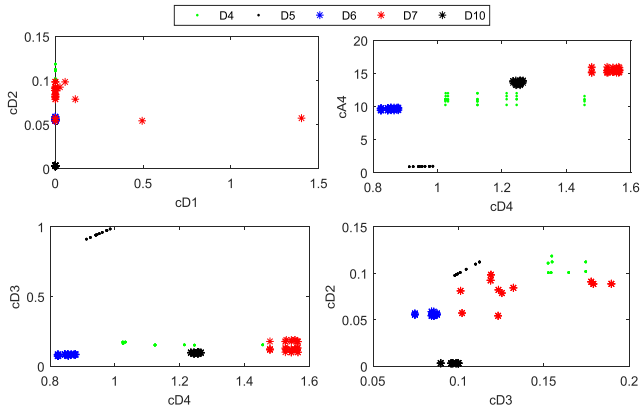

Fig. 15 Fuzzy c-means clustering of the single stage PQ disturbances of group G2 data (a) cD1-cD2 plot (b) cD4-cA4 plot (c) cD4-cD3 plot and (d) cD3-cD2 plot used for classification of disturbances.

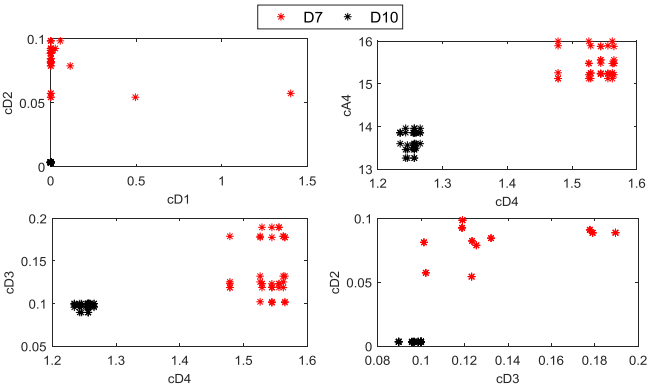

Fig. 16 Fuzzy c-means clustering of the single stage PQ disturbances of group G21 data (a) cD1-cD2 plot (b) cD4-cA4 plot (c) cD4-cD3 plot and (d) cD3-cD2 plot used for classification of disturbances.

The scatter plots of the disturbances related to the disturbances D4: Voltage Sag with Oscillatory Transient, D5: Momentary Interruption with Oscillatory Transient, D6: Harmonics with Oscillatory Transient included in the group G22 are provided in the Fig. 17. It is observed from the Fig. 17 that all the scatter plots are found to be effective in the classification of the disturbances D4: Voltage Sag with Oscillatory Transient, D5: Momentary Interruption with Oscillatory Transient, D6: Harmonics with Oscillatory Transient from each other.

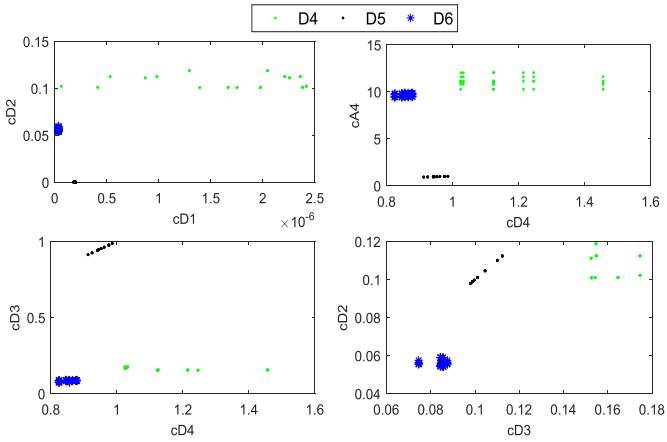

Fig. 17 Fuzzy c-means clustering of the single stage PQ disturbances of group G22 data (a) cD1-cD2 plot (b) cD4-cA4 plot (c) cD4-cD3 plot and (d) cD3-cD2 plot used for classification of disturbances.

VII. CONCLUSIONS

The proposed algorithm based on the discrete wavelet transform and Fuzzy C-means clustering has also been implemented for the recognition of the complex power quality disturbances. The complex power quality disturbances have been generated in MATLAB using the various combinations of the mathematical models of the single stage power quality disturbances such as voltage sag, voltage swell, momentary interruption, oscillatory transient, impulsive transient, harmonics, notch and spike. The voltage signals with complex PQ disturbances have been decomposed using the discrete wavelet transform and analyzed up to fourth level of decomposition. The plots related to the detail coefficients and approximation coefficients are used for the detection of complex PQ disturbances. The features extracted from the detail and approximation coefficients have been given as input to the Fuzzy c-means clustering for classification of the complex PQ disturbances. It has been concluded that the proposed algorithm based on the discrete wavelet transform and Fuzzy c-means clustering is effective in the recognition of the complex PQ disturbances.

REFERENCES

[1] Saurabh Kamble and Ishita Dupare, "Detection of power quality disturbances using Wavelet Transform and artificial neural network," International Conference on Magnetics, Machines & Drives, 2014.

[2] Om Prakash Mahela, Abdul Gafoor Shaik and Neeraj Gupta, "A critical review of detection and classification of power quality events," Renewable and Sustainable Energy Reviews, Vol. 41, pp. 495–505, 2015.

[3] Marcelo A.A. Lima, Augusto S. Cerqueira, Denis V. Courya and Carlos A. Duqueb, "A novel method for power quality multiple disturbance decomposition based on Independent Component Analysis," International Journal of Electrical Power and Energy Systems, vol. 42, pp. 593–604,June 2012.

[4] Rahul Dubey, S. R.Samantaray, B. Chitti Babu and S. Nandha Kumar, "Detection of power quality disturbances in presence of DFIG wind farm using Wavelet Transform based energy function," IEEE International Conference, 2011.

[5] Norman C.F.Tse, John Y.C.Chan, Wing-Hong Lau and Loi Lei Lai, "Hybrid Wavelet and Hilbert Transform with frequency-shifting decomposition for power quality analysis," IEEE Transactions on Instrumentation and Measurement , vol. 61, no. 12, pp-3225-3233, Dec 2012.

[6] E.A. Cano Plataa and H.E. Tacca, "Power load identification," Journal of the Franklin Institute, vol. 342, pp 97–113, AUG2004.

[7] Alireza Akhbardeha, Sakari Junnilaa, Mikko Koivuluomaa, Teemu Koivistoinenb, Vaino¨ Turjanmaab, Tiit Koobib and Alpo Varria, "Towards a heart disease diagnosing system based on force sensitive chair's measurement, biorthogonal wavelets and neural networks," Engineering Applications of Artificial Intelligence, vol. 20, pp. 493–502,Oct 2007.

[8] Zahra Moravej, Jamal Dehghani Ashkezari and Mohammad Pazoki, "An effective combined method for symmetrical faults identification during power swing," Electrical Power and Energy Systems, vol.64, pp. 24–34, July 2015.

[9] Tarun Kumar Chheepa, Tanuj Manglani, "Power Quality Events Classification using ANN with Hilbert Transform," IJMERT, Vol.6 , No.6 , pp.227-235, June 2017.

[10] Om Prakash Mahela, Abdul Gafoor Shaik, "Recognition of power quality disturbances using S-transform based ruled decision tree and fuzzy C-means clustering classifiers," Applied Soft Computing, Vol. 59, pp. 243–257, 2017.

